A Stroke Width Based Parameter-Free Document Binarization Method

Qiang Chen(✉), Qing Wang, Sheng-tao Lu, and Yu-ping Wang

School of Computer Science and Engineering,
Nanjing University of Science and Technology, Nanjing, China
chen2qiang@njust.edu.cn

Abstract. This paper presents a parameter-free document binarization method based on text characteristics. For a given stroke width, the text and background regions in binarized object regions are estimated with morphological operators. Then according to the numbers of the text and background pixels an optimal threshold is determined. To make the proposed method parameter-free, an automatic estimation of stroke width is also proposed based on the ratio of thick stroke pixels to binarized object pixels. Document images with various degenerations, such as stain and bleed-through, were used to test the proposed method. Comparison results demonstrate that our method can achieve a better performance than Otsu's, Kwon's, Chen's, Transition, and Moghaddam's binarization methods.

Keywords: Image binarization · Stroke width · Parameter-free

1 Introduction

Document image binarization is a classical method with a challenging problem. It is important for the Document Image Analysis and Retrieval (DIAR) community since it affects subsequent stages in the recognition process [1, 2]. For binarization, each pixel in a document image is classified as a foreground or a background pixel. State-of-the-art methods have been evaluated [1, 3], and all assume dark characters on bright background.

With dominant approach for document binarization [3], image thresholding, can be categorized into global and local classes. Five global thresholding algorithms were evaluated in [4]. Otsu [5] and Kittler and Illingworth [6] methods produced relatively good performance. Based on Otsu's method [5], several improved methods have been proposed for document binarization. These are: (1) Chen and Li [7] proposed a new discriminant criterion, which emphasizes much the homogeneity of the object gray level distribution and while intentionally de-emphasizes the heterogeneity of the background; (2) The two-distribution limit of Otsu's method was removed in [8], where the degradation modes on the histogram of the image are discarded one by one recursively applying Otsu's method until only one mode remains on the image; (3) AdOtsu, an adaptive modification of Otsu's method, was proposed in [9, 10] by introducing a multi-scale framework; (4) Wen et al. [11] presented a binarization method for non-uniform illuminated document images by combining the Curvelet transform and Otsu's method; (5) Ntirogiannis et al. [12] combined the Otsu and

Y.-J. Zhang (Ed.): ICIG 2015, Part I, LNCS 9217, pp. 480–493, 2015.
DOI: 10.1007/978-3-319-21978-3_42

Niblack methods for handwritten document images. The proposed method in this paper also belongs to a global thresholding algorithm, however the global threshold is determined by the numbers of the text and background pixels in the binarized object regions. Compared with Otsu's method, our method considers the stroke characteristics of document images.

Strokes are trajectories of a pen tip for document binarization, and the stroke width of handwritten or printed characters should be consistent. Based on the consistency of stroke width, several methods [8, 13–16] have been proposed for document image binarization. Liu and Srihari [13] presented a global thresholding algorithm with shape information. In logical level threshold method [14], stroke width is used as a pre-defined parameter. In adaptive logical level threshold method [15], stroke width is determined automatically before the binarization process and used subsequently to determine the size of the local windows. Ye et al. [8] proposed a stroke-model-based character extraction method for gray-level document images, which can detect thin connected components selectively, while ignoring relatively large backgrounds that appear complex. Shi et al. [16] presented a local threshold algorithm of document images by introducing the stroke width as shape information into local thresholding.

For the stroke based methods, the stroke width is an important parameter. In [8, 14], the stroke width is pre-defined. In [13, 15], run-length histogram was used to estimate the stroke width. A run in an image is a group of connected pixels containing the same grey-scale value, and the number of pixels in the run is defined as the run length and is used to select the threshold. Since run lengths are computed along x and y directions separately, it is not rotation invariant. Similar to the run-length histogram, Su et al. [17] introduced a stroke width estimation algorithm based on binary text stroke edge images. Instead of run-length histogram, the distance transform [18] is used to calculate stroke width [16]. This consists of two stages, namely training and testing. Moghaddam and Cheriet [9, 10] proposed a kernel-based algorithm to estimate the average stroke width. In measuring the frequency of different stroke width values, they computed the stroke width spectrum based on a rough binarization obtained with the grid-based Sauvola method [19]. Thus, the kernel-based algorithm is not robust because the rough binarization is not stable for degraded document images.

This paper presents an automatic stroke width estimation method based on the ratio change of thick stroke pixels that are false text pixels. This has the following advantages: rotation invariant, no training, and independent of a rough binarization. Based on the estimated stroke width an optimal global threshold is generated to obtain a binarization result. During the process of estimating stroke width and generating global threshold, there are no parameters to be set.

2 Stroke Width Based Parameter-Free Document Binarization

Assuming that the stroke width of characters is consistent, we present an automatic stroke width based document binarization algorithm. Figure 1 shows the flowchart of the proposed algorithm, where the constants $I_{\min}$ and $I_{\max}$ are the minimum and maximum gray intensity values of the denoised document image, respectively. In order

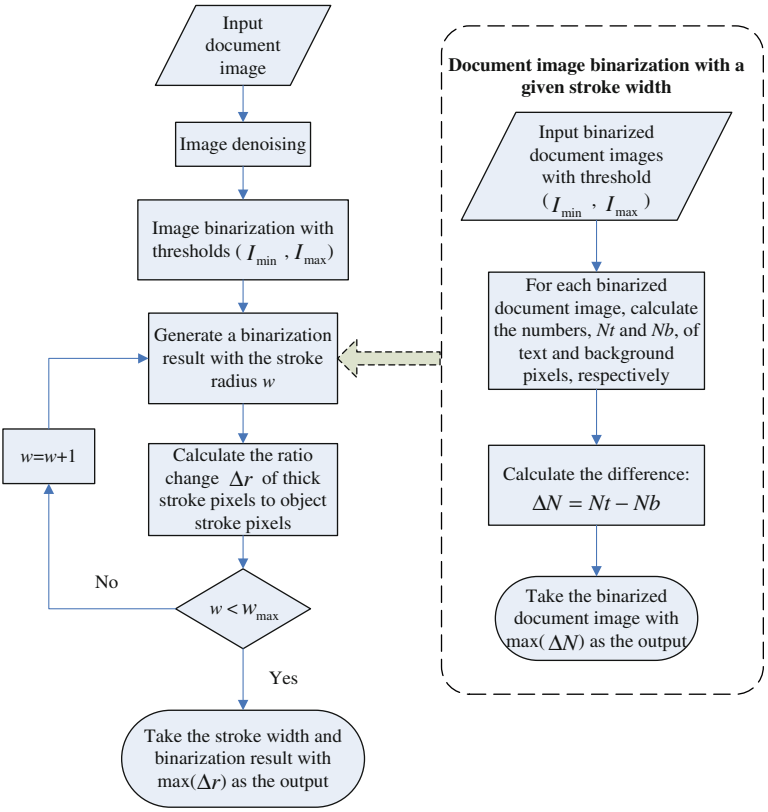

Fig. 1. Flowchart of the proposed algorithm

to suppress the noise influence, a Gaussian filter was used. The constant w_{max} represents the maximum stroke radius. The right part of Fig. 1 marked with the dashed frame represents the document image binarization with a given stroke width. The optimal threshold, to generate the binarized result with the given stroke width, is corresponding to the maximum difference between the numbers of text and background pixels. The estimated stroke width and final binarized result are corresponding to the maximum ratio change of thick stroke pixels to object stroke pixels. The left part of Fig. 1 is the main process of our algorithm, which includes the automatic estimation of the stroke width and the generation of a final binarization. In the proceeding sections, the right part of Fig. 1 will be described first.

2.1 Document Image Binarization with a Given Stroke Width

The basic idea of the proposed algorithm is to determine an optimal global threshold. The binarized threshold results revealed many text pixels with few background pixels. Stroke width is used to judge whether each binarized foreground pixel is a text or background pixel. For each foreground pixel, if the minimum distance from it to

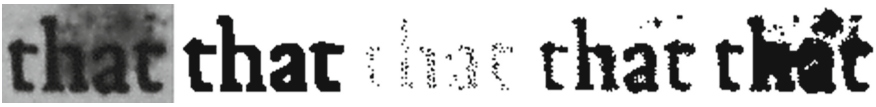

(a) Originalimage (b) Manualbinarization (c) Threshold 20 (d) Threshold 60 (e) Threshold 90

Fig. 2. Binarized results with different thresholds.

background regions is less than the stroke width, it is a text pixel; otherwise it is a background pixel. Figure 2 shows an example to demonstrate the basic idea. Figure 2 (b) is the manual binarization of an original text image (Fig. 2(a)), which is taken as the optimal binarized result. Figures 2(c)–(e) are three binarized results with three different thresholds (20, 60 and 90), respectively. From Fig. 2, we can observe that the threshold 20 is smaller than the optimal threshold because many text pixels are not in the foreground (or dark) region. The threshold 90 is larger than the optimal threshold because many background pixels are classified into the foreground region, which results in thick strokes. The threshold 60 is close to the optimal threshold because most of the text pixels are in the foreground region and a few of the background pixels are classified into the foreground region. In the following section, mathematical morphology is adopted to implement the basic idea.

Let I be an input document image, and $I_{\min}$ and $I_{\max}$ be the minimum and maximum gray intensity values of the document image, respectively. Then, the binarized image $B_i(i = 1, 2, \cdots, I_{\max} - I_{\min} - 1)$ is generated with a global threshold $t_I = I_{\min} + 1, \cdots, I_{\max} - 1$, where text (dark) and background (white) pixels are marked with 0 and 1, respectively. For each binarized image B_i, morphological operators are adopted to estimate the numbers of real and false object pixels. Let S_1 and S_2 be the disk-shaped structuring elements with the radius w and $w + 1$, respectively. The given stroke width is $2w + 1$ for the radius w. The structuring elements are generated with the Matlab function strel('disk', a, 4) where $a = w$ and $w + 1$. The thick object regions can be obtained with morphological closing:

$$TcO_k = (B_i \oplus S_k) \otimes S_k, \quad k = 1, 2 \tag{1}$$

where '$\oplus$' and '$\otimes$' denote image dilation and erosion operators, respectively. 'TcO_k' represents the thick object regions whose stroke radius is larger than w (or w + 1) for $k = 1, 2$, respectively. The reason of using two structuring elements is to make our algorithm suitable for document images where the text width has small difference. The thin object regions whose stroke radius is smaller than the given radius can be calculated by excluding the thick object regions from the original binarized image:

$$TnO_k = B_i \backslash TcO_k = \{x : x \in B_i, x \notin TcO_k\}, \quad k = 1, 2 \tag{2}$$

Then a mask for expanding text region is constructed as follows:

$$M = TnO_1 \otimes S_2 \tag{3}$$

The reason that we use TnO_1 (not TnO_2) in Eq. (3) is that there are less false object pixels in TnO_1 than in TnO_2. The reason that we use S_2 (not S_1) in Eq. (3) is the larger structuring element S_2 can generate the larger text expanding region. Using the mask, we restrict the thicker object region:

$$Mo = M \cap TnO_2 = \{x : x \in M, x \in TnO_2\} \tag{4}$$

In the restricted thicker objection region Mo, the object pixels connected with the thin object region TnO_1 are taken as the text pixels by seed filling, called as Tr. The final background region Br can be obtained as follows:

$$Br = B_i \backslash Tr = \{x : x \in B_i, x \notin Tr\} \tag{5}$$

Then, the numbers of object pixels in the text region Tr and the background region Br are denoted by Nt_i and Nb_i, respectively. The difference between Nt_i and Nb_i is

$$\Delta N_i = Nt_i - Nb_i \tag{6}$$

The threshold corresponding to the maximum ΔN is then taken as the optimal threshold in order to obtain the optimal binarization result. This is because the text pixels are abundant as compared to the background pixels using the threshold algorithm.

Figure 3 shows the process of a document image binarization with a given stroke width. Figure 3(b) is a binarized image with t_I = 80 of the original image Fig. 3(a). Figures 3(c) and (d) are two object regions whose stroke widths are larger than the 9 and 11 (here w = 4), respectively. The dark regions in Fig. 3(e) and (f) represent the thin object regions whose stroke widths are smaller than 9 and 11, respectively. Figure 3(h) is the restricted thicker object regions by combining Figs. 3(f) and (g), the text mask by eroding the thinner object regions Fig. 3(e). Figure 3(i) is the obtained text regions by taking Fig. 3(e) as the seeds and filling in Fig. 3(h). Figure 3(j) is the background regions by removing text regions Fig. 3(i) from the binarized object

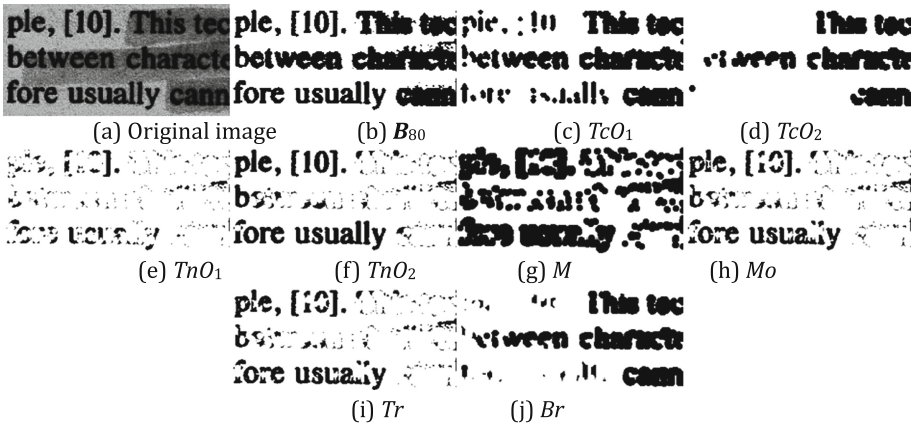

Fig. 3. Implement process of a document image binarization with a given stroke width

regions Fig. 3(b). Based on Fig. 3(i) and (j), the numbers of the text and background regions can be calculated. Figure 3 indicates that the threshold 80 is high because many background pixels are taken as object pixels and connected to the text regions. This thickens the text regions and makes them become background regions.

Figure 4 demonstrates the relationship between the difference ΔN and the threshold t_I for Fig. 3(a) when the radius of the stroke width is 4 pixels. It can be seen from Fig. 4 that ΔN increases when the threshold increases from 0 (I_{min}) to 28, and then decreases when the threshold increases from 28 to 194 (I_{max}). Since the intensity values of the text regions in Fig. 3(a) is smallest, the increased object regions mainly consist of the text regions for small thresholds. With the increasing of the threshold further, more and more background regions are contained in the object regions, and the number of the background regions is larger than that of the text regions when the threshold is larger than 64. The threshold corresponding to the maximum ΔN is 28, which is the optimal threshold for the given stroke width. The optimal threshold changes if stroke width is changed. In the following section, the automatic stroke width estimation method will be described.

2.2 Stroke Width Estimation

By increasing the stroke width, the estimated optimal threshold increases under the proposed algorithm. This is because more foreground pixels are introduced in the text regions. We assume that in a document image, the intensity distribution of text regions is relatively constant, and the intensity distribution of background regions has several relatively constant regions. Figure 5 shows an example, where Fig. 5(a) is the same as Fig. 3(a). The intensity distribution of the text regions is relatively constant because they are mainly located at the left part of the histogram as marked in Fig. 5(e). The intensity distribution of the background regions has two relatively constant ranges, as shown in Figs. 5(c)–(e). Therefore, a big change of the ratio of text pixels to the

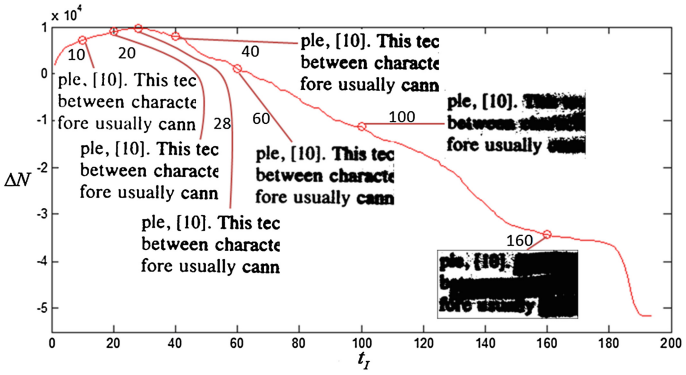

Fig. 4. Differences between the numbers of text and background regions for different threshold. Seven binarized images corresponding to seven red circle are attached. The numbers near the magenta lines are the thresholds of the seven binarized images (Color figure online).

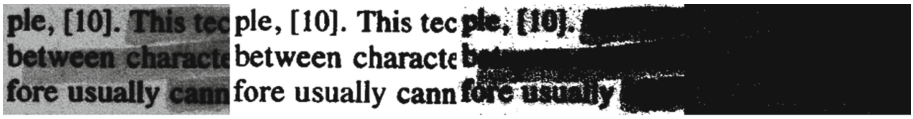

(a) Original image (b) Threshold 28 (c) Threshold 150 (d) Threshold 220

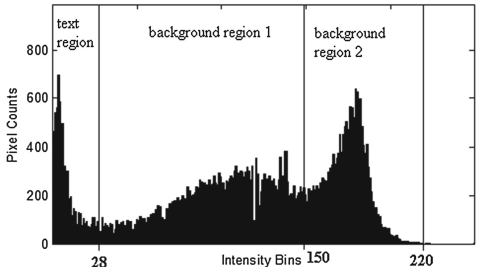

(e) Histogram

Fig. 5. Intensity distribution of a document image. (b)–(d) are three binarized images of the original image (a) with three thresholds 20, 150 and 220, respectively. (e) is the histogram of (a) where the positions of the three thresholds, and text and background regions are marked.

foreground pixels will occur with the increasing of the given stroke width. Based on the assumption above, we present a novel stroke width estimation method below.

Let the radius w of the stroke width range from 1 to $w_{\max}$, $w_{\max} = 10$ in this paper. For each radius w_i, $i = 1, \cdots, w_{\max} - 1$, we can obtain the binarized image Bt_i with the proposed method above. For each binarized image Bt_i, the framework F_i and edge image E_i of the object regions can be generated with morphological operators, Matlab functions bwmorph($\overline{Bt_i}$, 'thin') and bwmorph($\overline{Bt_i}$, 'remove'), respectively. $\overline{Bt_i}$ represents the inverted image of the binarized image Bt_i. The object and background regions in Matlab are marked as 1 and 0, respectively, which is contrary to our assumption in Sect. 2.1. Then, we calculate the minimum Euclidean distance D_j, $j = 1, \cdots, nF_i$, of each framework pixel to the edge image, where nF_i represents the number of the object pixels in the framework (F_i). The ratio of thick stroke pixels to the object pixels in the framework can be obtained:

$$r_i = \frac{nFt_i}{nF_i} \tag{7}$$

where nFt_i represents the number of thick stroke pixels (namely the minimum Euclidean distance is larger than w_i) in F_i. Then the change between two neighbor ratios of thick stroke pixels is

$$\Delta r_i = r_i - r_{i-1}, \quad i = 2, \cdots, w_{\max} - 1 \tag{8}$$

The stroke width and the binarized image corresponding to the maximum Δr are taken as the final stroke width and binarized result respectively.

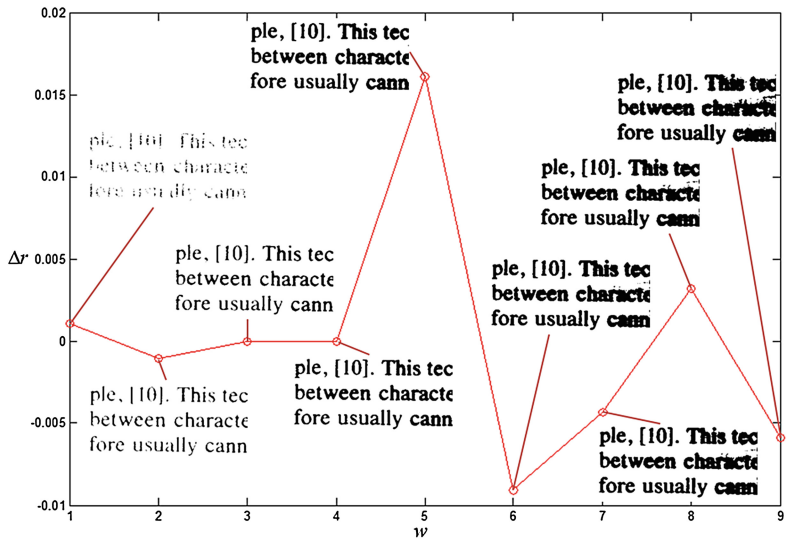

Fig. 6. Ratio change for each radius of the stroke width. Nine binarized images corresponding to nine red circle are attached (Color figure online).

Figure 6 shows the change in ratio of each stroke width is radius. Nine binarized images are attached where the original image is Fig. 3(a). It can be seen from Fig. 6 that the number of the object pixels in these binarized images increases with the increasing of the radius w. More text and background pixels are classified as the object regions. The binarized image corresponding to the maximum ratio change contains many of the text pixels, with no background pixels.

3 Experimental Results and Analysis

We compared the proposed method with Otsu's [5], Kwon's [20], Chen's [7], Transition [21], and Moghaddam's [9] methods. With the exception of the two parameter-free methods, that is the proposed and Kwon's methods, the parameters of the other four methods were set according to the default setting given in their literatures. Two images downloaded from internet and seven images from the document image binarization contest (DIBCO) 2009, 2010 and 2011 datasets[1] were used for qualitative and quantitative comparisons, respectively.

3.1 Qualitative Comparison

Figure 7 shows the binarization results of two images. For the first image, the proposed method obtained the best visual performance than the other methods. Many of the

[1] http://utopia.duth.gr/∼ipratika/DIBCO2011/resources.html.

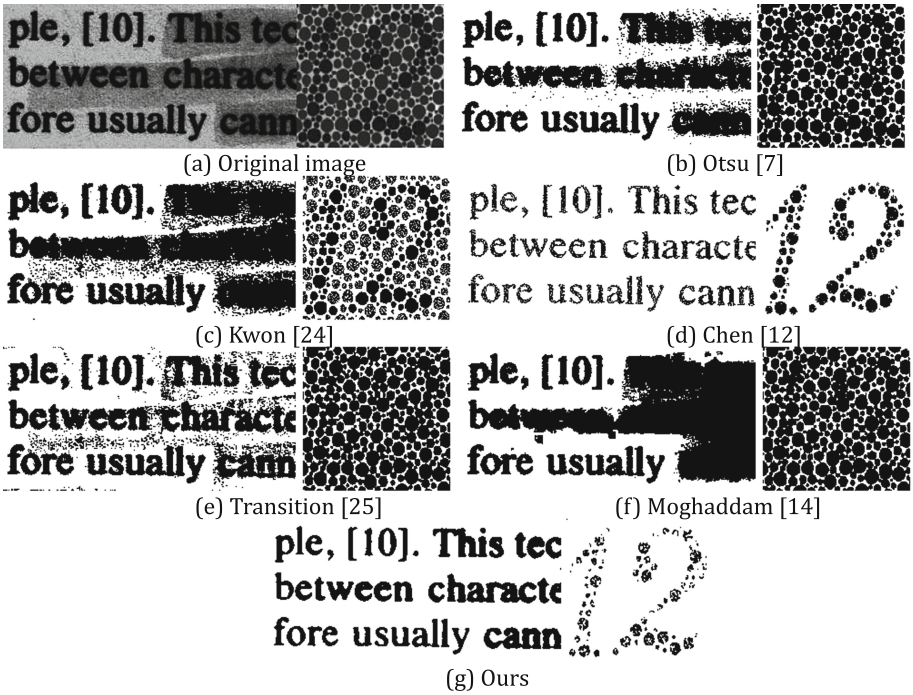

Fig. 7. Qualitative Comparison of two images

background were classified as object regions in Otsu's, Kwon's, Transition and Moghaddam's methods, while in Chen's method parts of the text regions were lost. For the second image, the number "12" immersed in the background can only be correctly extracted by the proposed method and Chen's method.

3.2 Quantitative Comparison

Figure 8 shows the three test images: a handwritten image with stains (Fig. 8a), a machine-printed image with texture backgrounds (Fig. 8b) and a handwritten image with bleed-through degradation (Fig. 8c). Various objective measures can be used to quantitatively evaluate the binarization performance. In this paper, the performance evaluations are based on the accuracy and F-measures.

The manual binarization result was used as the "gold standard". Pixels are classified into four categories: True Positive (TP), True Negative (TN), False Positive (FP), and False Negative (FN). TP and TN denote the number of pixels that are correctly binarized as foreground and background pixels, respectively. FP and FN are defined similarly. Then the formulations of the measures can be expressed as

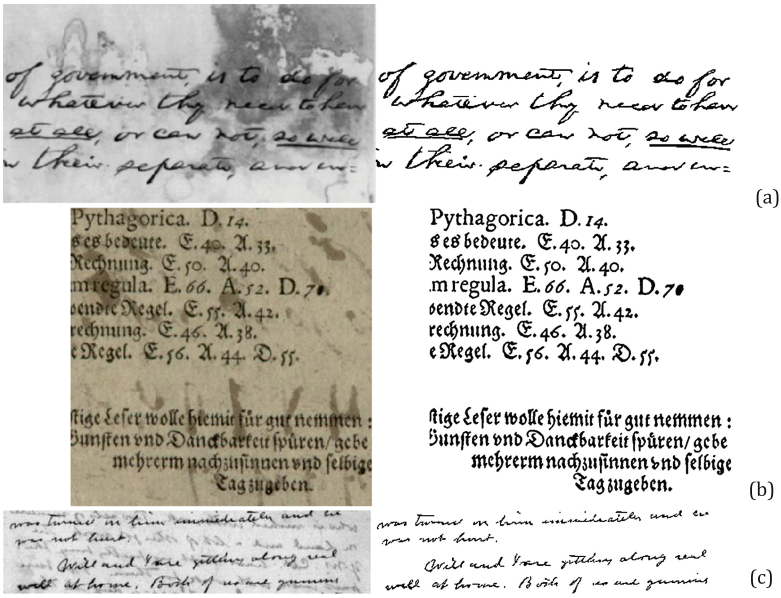

Fig. 8. Three original test images (left) and their corresponding gold standard images (right). (a) and (c) are two handwritten document images. (b) is a machine-printed document image.

$$Accuracy = \frac{TP + TN}{TP + FP + TN + FN} \tag{9}$$

$$F\text{-}measure = \frac{2 \times Recall \times Precision}{Recall + Precision} \tag{10}$$

Where $Recall = \frac{TP}{TP+FN}$, and $Precision = \frac{TP}{TP+FP}$.

Table 1 shows the accuracy and F-measure on the test images. Figures 9, 10 and 11 show the binarized results of Fig. 8(a)–(c), respectively. The proposed method can achieve the higher accuracy and F-measure for most of the test images than the other methods.

Table 1. Accuracy (Acc.) (Unit: %) and F-measure (Unit: %) on the test images

Method	Figure 8(a)		Figure 8(b)		Figure 8(c)	
	Acc.	F-measure	Acc.	F-measure	Acc.	F-measure
Otsu	78.77	40.56	93.37	79.98	98.51	88.28
Kwon	57.01	25.44	63.53	43.08	56.57	21.01
Chen	92.80	3.64	88.66	30.30	95.32	32.05
Transition	88.52	52.04	92.87	74.99	79.09	34.44
Moghaddam	79.90	41.65	91.93	76.24	98.70	89.61
Ours	96.44	74.56	95.66	89.61	98.73	87.86

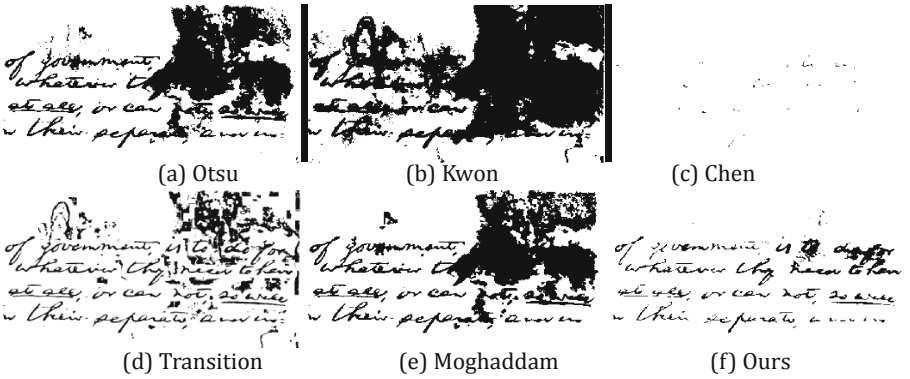

(a) Otsu (b) Kwon (c) Chen

(d) Transition (e) Moghaddam (f) Ours

Fig. 9. Binarized results of Fig. 8(a) with different methods

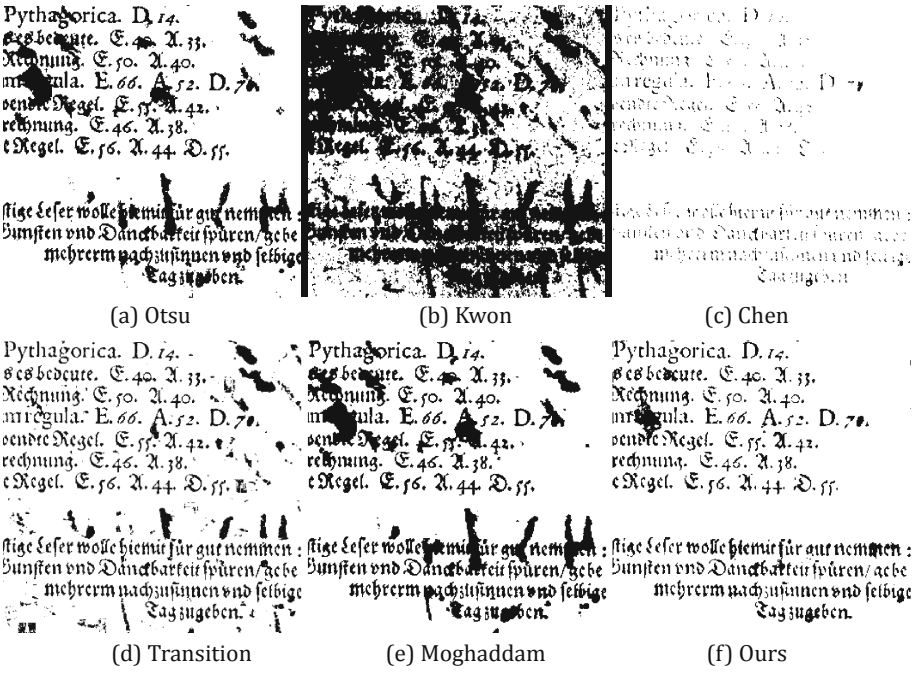

(a) Otsu (b) Kwon (c) Chen

(d) Transition (e) Moghaddam (f) Ours

Fig. 10. Binarized results of Fig. 8(b) with different methods

Aside the use of the three test images in Fig. 8, we also compared the performance of these methods with the whole handwritten five images from the DIBCO 2009 datasets. Table 2 shows the average accuracy and F-measure. Figure 12 shows the

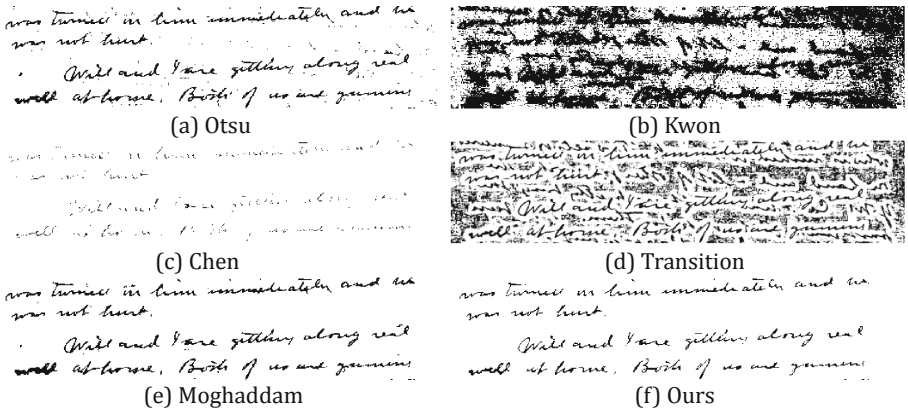

(a) Otsu (b) Kwon (c) Chen (d) Transition (e) Moghaddam (f) Ours

Fig. 11. Binarized results of Fig. 8(c) with different methods

Table 2. Average accuracy and F-measure (Unit: %) on DIBCO 2009 handwritten dataset

	Otsu	Kwon	Chen	Transition	Moghaddam	Ours
Accuracy	90.93	55.75	94.72	94.26	92.32	97.52
F-measure	65.94	20.82	24.20	63.70	68.71	76.09

quantitative comparison of the six methods on the test dataset, where the horizontal coordinates are corresponding to the five test images. Table 2 indicates that our method can achieve the highest average accuracy and F-measure than the other methods. By using Otsu's and Moghaddam's methods, it can be seen that image #2, are better compared to our method (Fig. 12). However, our method is the most stable and robust because it can obtain a relatively good binarized result for each test image.

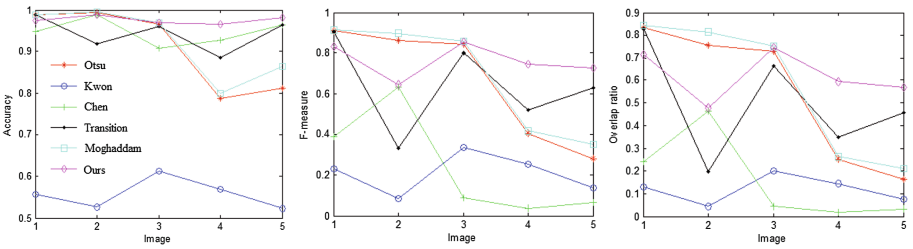

(a) Accuracy (b) F-measure (c) Overlap ratio

Fig. 12. Comparison of DIBCO 2009 handwritten dataset. In (a)–(c), the Otsu's, Kwon's, Chen's, Transition, Moghaddam's and Our methods are marked with the red, blue, green, black, cyan and magenta curves, respectively, as shown in (a) (Color figure online).

4 Limitations

Although the proposed method is usually effective for document images with various degenerations, such as stain and bleed-through, it has the following limitations: (1) Non-uniform illuminated document images. Since the proposed method is a global thresholding algorithm, a threshold cannot separate text and background regions for the degenerated document images with heavy non-uniform illumination. In order to make the proposed method suitable for non-uniform illuminated document images, non-uniform illumination correction, such as the Curvelet-based method [11], can be adopted before the binarization; and

(2) Document images with greatly different stroke width. We assume in the proposed method that the stroke width of characters is similar, no greatly difference. For the document images with the characters that whose stroke widths change greatly, a block-based strategy can be adopted. Firstly the document image is partitioned according to the height of characters. The stroke widths are similar in each block. Then the proposed method can be used for each block.

5 Conclusions

We present a novel parameter-free document binarization method based on stroke width, which mainly includes two novelties: (1) an automatic stroke width estimation algorithm is proposed based on the ratio of thick stroke pixels to binarized object pixels, which is rotation invariant and no training; and (2) under a given stroke width, an optimal threshold is determined according to the numbers of the text and background pixels in the binarized object regions.

During the process of stroke width estimation and optimal threshold determination, there is no need to set the parameters. The proposed method is evaluated qualitatively and quantitatively by comparing with other five binarization methods. The experimental results indicate that the proposed method can achieve a higher binarization accuracy for document images with various degenerations, such as stain, complex background and bleed-through. We also pointed out two limitations of our method, which are non-illumination and great change of stroke width. These can be solve by non-uniform illumination correction and block-based strategy, respectively.

Acknowledgments. This work was supported by the Fundamental Research Funds for the Central Universities under Grant no. 30920140111004, and the Six Talent Peaks Project in Jiangsu Province under Grant no. 2014-SWYY-024.

References

1. Pratikakis, I., Gatos, B., Ntirogiannis, K.: ICDAR 2011 document image binarization contest (DIBCO 2011). In: International Conference on Document Analysis and Recognition, pp. 1506–1510 (2011)

2. Lins, R.D., da Silva, J.M.M., Martins, F.M.J.: Detailing a quantitative method for assessing algorithms to remove back-to-front interference in documents. J. Univ. Comput. Sci. **14**(2), 266–283 (2008)
3. Trier, O.D., Jain, A.K.: Goal-directed evaluation of binarization methods. IEEE Trans. Pattern Anal. Mach. Intell. **17**(12), 1191–1201 (1995)
4. Lee, S.U., Chung, S.Y.: A comparative performance study of several global thresholding techniques for segmentation. Comput. Vis. Graph. Image Process. **52**, 171–190 (1990)
5. Otsu, N.: A threshold selection method from gray-scale histogram. IEEE Trans. Syst. Man Cybern. **8**, 62–66 (1978)
6. Kittler, J., Illingworth, J.: On threshold selection using clustering criteria. IEEE Trans. Syst. Man Cybern. **15**, 273–285 (1985)
7. Chen, S.C., Li, D.H.: Image binarization focusing on objects. Neurocomputing **69**, 2411–2415 (2006)
8. Ye, X., Cheriet, M., Suen, C.Y.: Stroke-model-based character extraction from gray-level document image. IEEE Trans. Image Process. **10**(8), 1152–1161 (2001)
9. Moghaddam, R.F., Cheriet, M.: A multi-scale framework for adaptive binarization of degraded document images. Pattern Recogn. **43**, 2186–2198 (2010)
10. Moghaddam, R.F., Cheriet, M.: AdOtsu: an adaptive and parameterless generalization of Otsu's method for document image binarization. Pattern Recogn. **45**, 2419–2431 (2012)
11. Wen, J.T., Li, S.M., Sun, J.D.: A new binarization method for non-uniform illuminated document images. Pattern Recogn. **46**(6), 1670–1690 (2013)
12. Ntirogiannis, K., Gatos, B., Pratikakis, I.: A combined approach for the binarization of handwritten document images. Pattern Recogn. Lett. **35**(1), 3–15 (2014)
13. Liu, Y., Srihari, S.N.: Document image binarization based on texture features. IEEE Trans. Pattern Anal. Mach. Intell. **19**(5), 540–544 (1997)
14. Kamel, M., Zhao, A.: Extraction of binary character/graphics images from grayscale document images. CVGIP: Graph, Models Image Process, 55, 203–217 (1993)
15. Yang, Y., Yan, H.: An adaptive logical method for binarization of degraded document images. Pattern Recogn. **33**, 787–807 (2000)
16. Shi, J., Ray, N., Zhang, H.: Shape based local thresholding for binarization of document images. Pattern Recogn. Lett. **33**, 24–32 (2012)
17. Su, B., Lu, S., Tan, C.L.: Robust document image binarization technique for degraded document images. IEEE Trans. Image Process. **22**(4), 1408–1417 (2013)
18. Borgefors, G.: Distance transformations in digital images. Comput. Vis. Graph. Image Process. **34**(3), 344–371 (1986)
19. Sauvola, J., Pietikinen, M.: Adaptive document image binarization. Pattern Recogn. **33**(2), 225–236 (2000)
20. Kwon, S.H.: Threshold selection based on cluster analysis. Pattern Recogn. Lett. **25**(9), 1045–1050 (2004)
21. Ramírez-Ortegón, M.A., Tapia, E., Ramírez-Ramírez, L.L., Rojas, R., Cuevas, E.: Transition pixel: a concept for binarization based on edge detection and gray-intensity histograms. Pattern Recogn. **43**, 1233–1243 (2010)